

D. A. Artemenkov · A. A. Bezbakh · V. Bradnova · V. Chudoba · M. S. Golovkov  
A. V. Gorshkov · Al-Z. Farrag · G. Kaminski · N. K. Kornegrutsa · S. A. Krupko  
K. Z. Mamatkulov · R. R. Kattabekov · V. V. Rusakova · R. S. Slepnev · R. Stanoeva  
S. V. Stepantsov · A. S. Fomichev · P. I. Zarubin · I. G. Zarubina

## $^8\text{He}$ Nuclei Stopped in Nuclear Track Emulsion

Received: 10 December 2013 / Accepted: 1 April 2014 / Published online: 19 April 2014  
© Springer-Verlag Wien 2014

**Abstract** A nuclear track emulsion (NTE) is exposed to 60 MeV  $^8\text{He}$  nuclei. Measurements of decays of  $^8\text{He}$  nuclei stopped in NTE allow one to evaluate possibilities of  $\alpha$ -spectrometry. Thermal drift of  $^8\text{He}$  atoms is observed. Knowledge of the energy and emission angles of  $\alpha$ -particles allows one to derive the energy distribution of  $\alpha$ -decays  $Q_{2\alpha}$ . The presence of a “tail” of large values  $Q_{2\alpha}$  is established.

### 1

There is a possibility to study  $2\alpha$ - and  $3\alpha$ -particle decays of some light nuclei by implanting them into a detector [1–5]. In this respect, nuclear track emulsion (NTE) is worthy to be used as well. The advantages of the NTE technique are the best spatial resolution (about 0.5  $\mu\text{m}$ ), the possibility of observing the tracks in a full solid angle and a sensitivity starting with relativistic particles. In NTE, the directions and ranges of the beam nuclei, as well as slow products of their decays can be measured, which provides a basis for spectrometry. Indeed, hammer-like tracks from decays of  $^8\text{Be}$  nuclei in the state  $2^+$  were observed in the  $\beta$ -decays  $^8\text{Li}$  and  $^8\text{Be}$  fragments stopped in NTE, which in turn were produced by high-energy particles [6]. Another example is the first observation of the  $^9\text{C}$  nucleus from the decay  $2\alpha + p$  [7]. Nowadays, when used with sufficiently pure secondary beams, NTE appears to be an effective means for studies of such decays.

Exposure of NTE to nuclei  $^8\text{He}$  of energy of 60 MeV [8] is performed at the fragment separator ACCULINNA [9] in the G. N. Flerov Laboratory of Nuclear Reactions, JINR. Features of decays of the  $^8\text{He}$  isotope are shown in Fig. 1, according to the compilation [10]. Figure 2 shows a mosaic macrophotograph of a decay of a nucleus  $^8\text{He}$  stopped in NTE. It is typical one among thousands observed in this study. Video recordings of such decays taken with the microscope and camera are collected [11].

---

D. A. Artemenkov (✉) · A. A. Bezbakh · V. Bradnova · V. Chudoba · M. S. Golovkov · A. V. Gorshkov · Al-Z. Farrag  
G. Kaminski · N. K. Kornegrutsa · S. A. Krupko · K. Z. Mamatkulov · R. R. Kattabekov · V. V. Rusakova · R. S. Slepnev  
R. Stanoeva · S. V. Stepantsov · A. S. Fomichev · P. I. Zarubin · I. G. Zarubina  
Joint Institute for Nuclear Research, Dubna, Moscow Region, Russia  
E-mail: artemenkov@lhe.jinr.ru

V. Chudoba  
Institute of Physics, Silesian University in Opava, Opava Czech Republic

G. Kaminski  
Institute of Nuclear Physics, PAN, Kraków, Poland

R. Stanoeva  
South West University, Blagoevgrad, Bulgaria

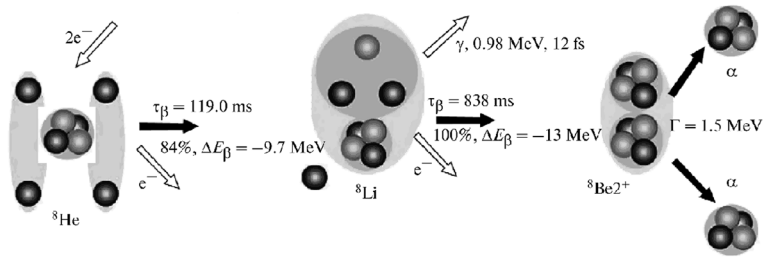


**Fig. 1** Scheme of a major channel of the cascade decay of  $^8\text{He}$  isotope; *light circles* correspond to protons, *dark ones* neutrons

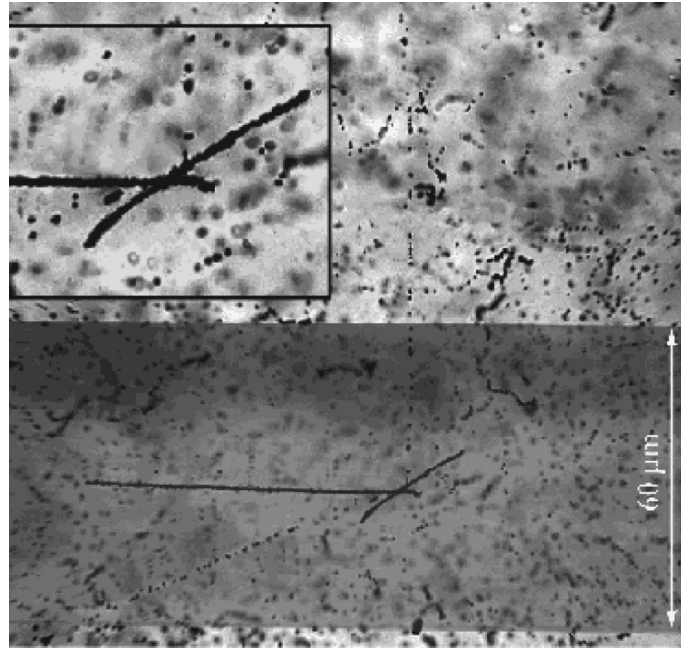


**Fig. 2** Mosaic macrophotography of a hammer-like decay of  $^8\text{He}$  nucleus (*horizontal track*) stopped in nuclear track emulsion. Pair of electrons (point-like tracks) and pair of  $\alpha$ -particles (short opposite tracks). On insertion (*top*): enlarged decay vertex. To illustrate spatial resolution the image of the decay is superimposed to macrophotography of a human hair of thickness of  $60\ \mu\text{m}$

When scanning the NTE pellicle with a  $20\times$  objectives on the microscopes MBI-9 a primary search for  $\beta$ -decays of  $^8\text{He}$  nuclei was focused on hammer-like events (Fig. 2). Often, in the events named “broken” ones gaps were observed between stopping points of primary tracks and subsequent hammer-like decays. In total 1413 “whole” and 1123 “broken” events were found. Decay vertices of 580 “broken” events were found to be laying in a backward hemisphere with the respect to arrival directions of ions. Corresponding to a half of the statistics this number indicate that the forward-backward asymmetry is absent. The “broken” events were attributed to a drift of thermalized  $^8\text{He}$  atoms that arose as a result of neutralization of  $^8\text{He}$  nuclei.

Arrival directions and stopping points of ions  $^8\text{He}$ , their decay vertices and stops of decay  $\alpha$ -particles were determined for 136 “whole” and 142 “broken” events. In “broken” events the decay points were determined by extrapolating the electron tracks. The distribution of the opening angles of  $\alpha$ -particle pairs  $\Theta_{2\alpha}$  has a mean value  $(164.9 \pm 0.7)^\circ$  at rms  $(11.6 \pm 0.5)^\circ$ . Some kink of “hammers” is defined by the momenta carried away by  $e\nu$ -pairs. The dependence of the  $\alpha$ -particle ranges and their energy values are determined by spline interpolation of calculations in the SRIM model [12]. The mean value of the  $\alpha$ -particle ranges is  $(7.4 \pm 0.2)\ \mu\text{m}$  at rms  $(3.8 \pm 0.2)\ \mu\text{m}$  corresponding to their mean energy  $(1.70 \pm 0.03)\ \text{MeV}$  at rms  $0.8\ \text{MeV}$ . Correlation of ranges of  $\alpha$ -particles in pairs is clearly manifested. The distribution of the range differences has rms  $2.0\ \mu\text{m}$ .

Knowledge of the energy and emission angles of  $\alpha$ -particles allows one to derive the energy distribution of  $\alpha$ -decays  $Q_{2\alpha}$ . The invariant variable  $Q$  is defined as the difference between the invariant mass of a final system  $M^*$  and the mass of a primary nucleus  $M$ , that is,  $Q = M^* - M$ ,  $M^*$  is defined as the sum of all products of the 4-momenta  $P_i$  of fragments, that is,  $M^{*2} = (\sum P_i)^2$ . In a case of an  $\alpha$ -particle pair  $i$  is equal just 1 and

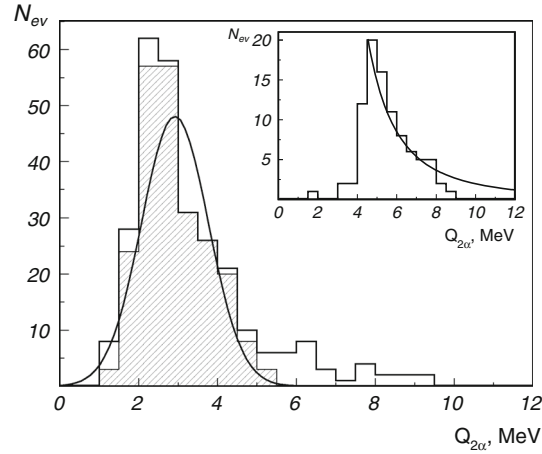


**Fig. 3** Distribution on energy  $Q_{2\alpha}$  of 278 pairs of  $\alpha$ -particles; hatched histogram correspond to condition of selection of events  $L_1$  and  $L_2 < 12.5 \mu\text{m}$ ,  $\Theta > 145^\circ$ ; line Gaussian. On the *insertion*:  $Q_{2\alpha}$  distribution of additional 98  $\alpha$ -pairs having  $L_1$  and  $L_2 > 12.5 \mu\text{m}$

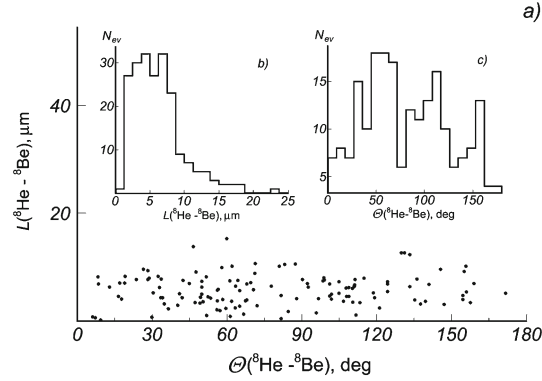


**Fig. 4** Distribution of the distances  $L(^8\text{He}-^8\text{Be})$  between the stopping points of the  $^8\text{He}$  ions and the decay vertices versus the angles  $\Theta(^8\text{He}-^8\text{Be})$  between directions of arrivals of the ions and directions from the stopping points of the ions to the decay vertices (a); insertions: projected histograms for  $L(^8\text{He}-^8\text{Be})$  (b) and  $\Theta(^8\text{He}-^8\text{Be})$  (c)

2. In general, the distribution of  $Q_{2\alpha}$  (Fig. 3) corresponds to the  $^8\text{Be}$  decay from the state  $2^+$ . However, the mean value of  $Q_{2\alpha}$  is slightly higher than expected. This fact is determined by the presence of a “tail” of large values  $Q_{2\alpha}$ , obviously not matched the description by a Gaussian function. Application of the selection criteria for both  $\alpha$ -particle ranges  $< 12.5 \mu\text{m}$  and opening angles  $\Theta > 145^\circ$ , provides a mean value of  $Q_{2\alpha}$  equal to  $(2.9 \pm 0.1) \text{ MeV}$  at rms  $(0.85 \pm 0.07) \text{ MeV}$ , which corresponds to the  $2^+$  state.

The measurements are continued to saturate statistics in the high energy “tail” of  $Q_{2\alpha}$ . The insertion in Fig. 3 shows  $Q_{2\alpha}$  with additional 98  $\alpha$ -pairs having both ranges above  $12.5 \mu\text{m}$ . It should be noted that the highly energetic  $\alpha$ -pairs are among better measurable ones despite to relatively rare appearance. The physical reason for the appearance of the “tail” in the distribution  $Q_{2\alpha}$  is not clear. Probably, its shape will allow one to verify calculations of spatial structure of 8-nucleon ensembles emerging as  $\alpha$ -pairs of the  $2^+$  state decays [13].

In the 142 “broken” events the distances  $L(^8\text{He}-^8\text{Be})$  between the stopping points of the  $^8\text{He}$  ions and the decay vertices as well as the angles  $\Theta(^8\text{He}-^8\text{Be})$  between directions of arrivals of the ions and directions from the stopping points of the ions towards the decay vertices are defined (Fig. 4). Uniformity of distributions of events over these parameters and absence of a clear correlation indicate on a thermal drift of the atoms  $^8\text{He}$ . The mean value of  $L(^8\text{He}-^8\text{Be})$  amounting to  $(5.8 \pm 0.3) \mu\text{m}$  at rms  $(3.1 \pm 0.2) \mu\text{m}$ , can be associated with a mean range of atoms  $^8\text{He}$ . The low value of a mean speed of the atoms  $^8\text{He}$  defined as ratio of the mean value of  $L(^8\text{He}-^8\text{Be})$  to the half-life of the nucleus  $^8\text{He}$  supports a pattern of diffusion.

Observation of the diffusion points to the possibility of generating of radioactive atoms  $^8\text{He}$  and pumping them out of sufficiently thin targets. Increasing of the mean speed and drift length is achievable due to heating

of the target. There is a prospect of accumulating of a significant amount of  $^8\text{He}$  atoms. In particular, a  $^8\text{He}$  radioactive gas can be used to measure the half-life of the  $^8\text{He}$  nucleus at a new level of precision and for laser spectroscopy of this isotope. Applied interest consists in studies of thin films by pumping atoms  $^8\text{He}$  and their deposition on  $\alpha$ -detectors. Such opportunities are developing intensively with respect of the  $^6\text{He}$  isotope [14, 15].

The practical result of this work is the demonstration of the opportunities of recently reproduced NTE in a way of exposure in a beam of  $^8\text{He}$  nuclei. Nuclear track emulsion made it possible to identify decays of stopped  $^8\text{He}$  nuclei, estimate possibilities of  $\alpha$ -range spectrometry and observe the drift of  $^8\text{He}$  atoms. The high quality of the beam of radioactive  $^8\text{He}$  nuclei at the ACCULINNA fragment separator was confirmed. The presented analysis of the decay of nuclei  $^8\text{He}$  can serve as a prototype for studying the decays of stopped nuclei  $^8,^9\text{Li}$ ,  $^8,^{12}\text{B}$ ,  $^9\text{C}$  and  $^{12}\text{N}$ . Statistics of hammer-like decays found in this study is a small part of the flux of  $^8\text{He}$  nuclei, and the measured decays—about 10% of this share. This limitation is defined by “reasonable expenses” of human time and labor. However, NTE in which radioactive nuclei are implanted provides a basis for the application of automated microscopy and image recognition software, allowing one to rely on unprecedented statistics. Thus, a synergy of classical technique and modern technology can be achieved.

**Acknowledgments** This work was supported by the Grants 12-02-00067, 11-02-00657 and 11-02-00657a of the Russian Foundation for Basic Research and grants of Plenipotentiary representatives of Bulgaria, Egypt and Romania at JINR.

## References

1. Miernik, K., et al.: Optical Time Projection Chamber for imaging nuclear decays. *Nucl. Instrum. Methods A* **581**, 194 (2007)
2. Mianowski, S., et al.: Imaging the decay of  $^8\text{He}$ . *Acta Phys. Pol. B* **41**, 449 (2010)
3. Hyldegaard, S., et al.: Precise branching ratios to unbound  $^{12}\text{C}$  states from  $^{12}\text{N}$  and  $^{12}\text{B}$   $\beta$ -decays. *Phys. Lett. B* **678**, 459 (2009)
4. Hyldegaard, S., et al.: Branching ratios in the beta decays of N-12 and B-12. *Phys. Rev. C* **80**, 044304 (2009)
5. Hyldegaard, S., et al.: R-matrix analysis of the beta decays of N-12 and B-12. *Phys. Rev. C* **81**, 024303 (2010)
6. Powell, C.F., Fowler, P.H., Perkins, D.H.: *The Study of Elementary Particles by the Photographic Method*. Pergamon Press, New York (1959)
7. Swami, M.S., et al.: Beta decay of a  $\text{C}^9$  nucleus. *Phys. Rev.* **103**, 1134 (1956)
8. Artemenkov, D. A., et al.: Exposure of nuclear track emulsion to  $^8\text{He}$  nuclei at the ACCULINNA separator. *Phys. Part. Nucl. Lett.* **10**, 415 (2013) [arXiv:1309.4808](https://arxiv.org/abs/1309.4808)
9. Rodin, A.M., et al.: Status of ACCULINNA beam line. *Nucl. Instrum. Methods B* **204**, 114 (2003)
10. Ajzenberg-Selove, F.: Energy levels of light nuclei  $A = 510$ . *Nucl. Phys. A* **490**, 1 (1988)
11. Web site of the BECQUEREL Project. <http://becquerel.jinr.ru> (2013)
12. Ziegler J.F., et al.: *SRIM: the stopping and range of ions in matter* (SRIM Co, ISBN 0-9654207-1-X, 2008). <http://srim.org/>
13. Wiringa, R.B., et al.: Quantum Monte Carlo calculations of  $A=8$  nuclei. *Phys. Rev. C* **62**, 014001 (2000)
14. Knecht, A., et al.: Precision measurement of the  $^6\text{He}$  half-life and the weak axial current in nuclei. *Phys. Rev. C* **86**, 035506 (2012)
15. Stora, T., et al.: A high intensity  $^6\text{He}$  beam for the beam neutrino oscillation facility. *Eur. Lett.* **89**, 32001 (2012)